

## High-speed solid state fluorination of Nb<sub>2</sub>O<sub>5</sub> yields NbO<sub>2</sub>F and Nb<sub>3</sub>O<sub>7</sub>F with photocatalytic activity for oxygen evolution from water

Martin Alexander Lange,<sup>1</sup> Ibrahim Khan,<sup>2,4</sup> René Dören,<sup>1</sup> Muhammad Ashraf,<sup>3</sup> Ahsanulhaq Qurashi,<sup>4,7</sup> Leon Prädel,<sup>5</sup> Martin Panthöfer,<sup>1</sup> Marcus von der Au,<sup>6</sup> Antje Cossmer,<sup>6</sup> Jens Pfeifer,<sup>6</sup> Björn Meermann,<sup>6</sup> Mihail Mondeshki,<sup>1</sup> Muhammad Nawaz Tahir,<sup>3\*</sup> and Wolfgang Tremel<sup>1\*</sup>

<sup>1</sup> Department Chemie, Johannes Gutenberg-Universität Mainz, Duesbergweg 10-14, D-55128 Mainz, Germany

<sup>2</sup> present address: Center of Integrative Petroleum Research, King Fahd University of Petroleum & Minerals, Dhahran 31261, Saudi Arabia

<sup>3</sup> Chemistry Department, King Fahd University of Petroleum & Materials, Dhahran 31261, P.O. Box 5048, Kingdom of Saudi Arabia

<sup>4</sup> Center of Excellence in Nanotechnology, King Fahd University of Petroleum & Minerals, Dhahran, 31262, Saudi Arabia

<sup>5</sup> Max Planck Institute for Polymer Research, Ackermannweg 10, 55128 Mainz, Germany

<sup>6</sup> Bundesanstalt für Materialforschung und -prüfung (BAM), Anorganische Spurenanalytik, Richard-Willstätter-Straße 11, D-12489 Berlin, Germany

<sup>7</sup> present address: Department of Chemistry, Main Campus, Khalifa University Abu Dhabi, 127788, UAE.

## Contents

Tables		
<b>Table S1</b>	Results of Rietveld-refinement of Nb <sub>3</sub> O <sub>7</sub> F and NbO <sub>2</sub> F synthesized by SPS ( <b>Figure 2A and B</b> ) and by conventional high temperature chemistry ( <b>Fig. S1A and B</b> )	page S2
<b>Table S2</b>	Experimental and theoretical fluorine concentration (pure phases) and degree of fluorination for niobium oxyfluorides prepared by SPS and conventional high temperature chemistry as determined by HR-CS-GFMAS.	page S3
<b>Table S3</b>	Summary of elemental compositions and calculated F/O surface ratios determined by XPS spectroscopy from <b>Fig. 4</b> and <b>Fig. S5</b>	page S4
<b>Table S4</b>	Fit parameters of the deconvoluted signals from the F <sup>-</sup> solid state MAS NMR of Nb <sub>3</sub> O <sub>7</sub> F and NbO <sub>2</sub> F prepared by SPS and conventional chemistry ( <b>Fig. S2</b> )	page S5
<b>Table S5</b>	Calculated Band edge position.	Page S6
Figures		
<b>Fig. S1</b>	Rietveld refinement of conventionally prepared NbO <sub>2</sub> F ( <b>A</b> ) and Nb <sub>3</sub> O <sub>7</sub> F ( <b>B</b> ).	page S7
<b>Fig. S2</b>	( <b>A-C</b> ) (HR)TEM images of Nb <sub>3</sub> O <sub>7</sub> F prepared by SPS, ( <b>D-F</b> ) and conventional chemistry. ( <b>A, D</b> ) show representative particles, ( <b>B, E</b> ) show a zoom view on edges of the particles, ( <b>C, F</b> ) show magnified crystalline areas and their respective Fourier transformation as insets.	Page S8
<b>Fig. S3</b>	Line Defects as observed via TEM in all synthesized sample powders	page S9
<b>Fig. S4</b>	XPS survey spectra of NbO <sub>2</sub> F and Nb <sub>3</sub> O <sub>7</sub> F synthesized by SPS ( <b>A, B</b> ) and conventional chemistry ( <b>C, D</b> ).	page S10
<b>Fig. S5</b>	XPS fine spectra of F, O, and Nb areas for Nb <sub>3</sub> O <sub>7</sub> F prepared by SPS ( <b>A-C</b> ) and conventional ampoule chemistry ( <b>D-F</b> ) with fitted peaks for the respective environments.	page S11
<b>Fig. S6</b>	Kubelka-Munk plots of NbO <sub>2</sub> F and Nb <sub>3</sub> O <sub>7</sub> F prepared by SPS ( <b>A-B</b> ) and conventional ampoule chemistry ( <b>C-D</b> ) from UV-Vis diffuse reflectance spectra ( <b>Figure 5A</b> ).	page S12
<b>Fig. S7</b>	<sup>19</sup> F MAS-NMR spectra of NbO <sub>2</sub> F ( <b>A</b> ) and Nb <sub>3</sub> O <sub>7</sub> F ( <b>B</b> ).	page S13
<b>Fig. S8</b>	Graphical representation of the theoretical and calculated band edge positions as listed in Table S5.	Page S14

**Table S1.** Results of Rietveld refinements of Nb<sub>3</sub>O<sub>7</sub>F (*Cmmm*) and NbO<sub>2</sub>F (*Pm-3m*) synthesized by SPS (Fig. 2A and 2B) and by conventional high temperature chemistry (Fig. S1). Because of large strain along long axis, conventionally prepared Nb<sub>3</sub>O<sub>7</sub>F was taken as reference for phase refinement. Phase-purity was assumed.

Sample	unit cell parameters			gof	R <sub>wp</sub>	Space group	Side phase	% side phase
	a	b	c					
NbO <sub>2</sub> F - SPS	3.9049(8)	-	-	3.61	3.89	<i>Pm-3m</i>	Nb <sub>3</sub> O <sub>7</sub> F	1.3 ± 0.1 %
Nb <sub>3</sub> O <sub>7</sub> F - SPS	20.693(2)	3.8387(3)	3.9383(3)	5.92	7.14	<i>Cmmm</i>	Nb <sub>3</sub> O <sub>7</sub> F	1.8 ± 0.2 %
NbO <sub>2</sub> F	3.898(1)	-	-	1.27	5.76	<i>Pm-3m</i>	Nb <sub>3</sub> O <sub>7</sub> F	17.4 ± 0.5 %
Nb <sub>3</sub> O <sub>7</sub> F	20.677(2)	3.8316(3)	3.9237(3)	2.48	4.30	<i>Cmmm</i>	-	0% assumed

**Table S2.** Experimental and theoretical fluorine concentration (pure phases) and degree of fluorination for niobium oxyfluorides prepared by SPS and conventional high temperature chemistry as determined by HR-CS-GFMAS.

SPS Sample	Fluorine conc. <i>via</i> HR-CS-GFMAS (g kg <sup>-1</sup> ± sd*)	theor. Fluorine conc. (g kg <sup>-1</sup> )	Niobium conc. <i>via</i> HR-CS-GFMAS (g kg <sup>-1</sup> ± sd*)	theor. Niobium conc. (g kg <sup>-1</sup> )
NbO <sub>2</sub> F - SPS	125 ± 9*	132	648 ± 18*	645
Nb <sub>3</sub> O <sub>7</sub> F - SPS	44 ± 10*	46	547 ± 13*	680

\*n = 3

**Table S3.** Summary of elemental compositions and calculated F/O surface ratios as determined by XPS spectroscopy.

<b>Sample</b>	<b>F 1s %</b>	<b>O 1s %</b>	<b>Nb 4f %</b>	<b>F : O ratio</b>
NbO <sub>2</sub> F - SPS	17.6	66.8	15.6	1 : 4
Nb <sub>3</sub> O <sub>7</sub> F - SPS	12.0	70.9	17.7	1 : 6
NbO <sub>2</sub> F	12.3	77.7	10.0	1 : 6
Nb <sub>3</sub> O <sub>7</sub> F	9.9	78.4	11.6	1 : 8
Nb <sub>2</sub> O <sub>5</sub>	0.0	80.3	12.9	/

**Table S4.** Fit parameters of the five deconvoluted peaks from the F<sup>-</sup> solid state MAS NMR of Nb<sub>3</sub>O<sub>7</sub>F (conventionally (bottom) and SPS-prepared (top), Figure S2A) and NbO<sub>2</sub>F (conventionally (bottom) and SPS-prepared (top), Figure S2B).

<b>NbO<sub>2</sub>F - SPS (Fig. S6B)</b>	<b>Peak 1</b>	<b>Peak 2</b>	<b>Peak 3</b>
Peak position / Hz	-11.28	-19.66	-27.17
FWHM / Hz	6.02	2.57	6.02
Relative peak area	12.31	78.41	9.28
<b>Nb<sub>3</sub>O<sub>7</sub>F - SPS (Fig. S6A)</b>	<b>Peak 1</b>	<b>Peak 2</b>	<b>Peak 3</b>
Peak position / Hz	-9.89	-21.05	-31.86
FWHM / Hz	3.38	3.74	4.51
Relative peak area	5.87	86.42	7.70
<b>NbO<sub>2</sub>F (Fig. S6B)</b>	<b>Peak 1</b>	<b>Peak 2</b>	<b>Peak 3</b>
Peak position / Hz	-12.39	-21.73	-28.50
FWHM / Hz	4.51	3.76	2.78
Relative peak area	15.85	68.01	16.14
<b>Nb<sub>3</sub>O<sub>7</sub>F (Fig. S6A)</b>	<b>Peak 1</b>	<b>Peak 2</b>	<b>Peak 3</b>
Peak position / Hz	-18.99	-22.60	-29.33
FWHM / Hz	3.38	1.92	3.38
Relative peak area	36.62	56.66	6.73

## Calculation of theoretical optical band positions

The conduction band ( $E_{CB}$ ) and valence band ( $E_{VB}$ ) potentials of semiconductors can be calculated using the following empirical equations.<sup>1,2,3</sup>

$$E_{CB} = \chi - E_e - \frac{1}{2} E_g$$

$$E_{VB} = E_{CB} + E_g$$

Here,  $E_{VB}$  are the valence band potential and  $E_{CB}$  the conduction band potential,  $E_e$  is the energy of free electrons on the hydrogen scale (4.5 eV),  $E_g$  is the band gap of the respective semiconductor and  $\chi$  stands for the absolute electronegativity of the atom semiconductor (geometric mean of the absolute electronegativity of the constituent atoms) and is calculated according to

$$\chi = [\chi(A)^a \times \chi(B)^b \times \chi(C)^c]^{1/(a+b+c)}$$

where  $a$ ,  $b$ ,  $c$  are the numbers of the elements  $A$ ,  $B$ ,  $C$  in the chemical formular of the semiconductor. The values listed in Table S5 were obtained from this equation. They are plotted in Fig. S8.

**Table S5.** Calculated band edge position values.

Semiconductor	Absolute electronegativity ( $\chi$ )	Energy of free electrons (hydrogen scale)	Band gap value ( $E_g$ )	Conduction band potential ( $E_{CB}$ )	Valence band potential ( $E_{VB}$ )
NbO <sub>2</sub> F - SPS	6.90	4.5 eV	3.29 eV	0.76 eV	4.05 eV
Nb <sub>3</sub> O <sub>7</sub> F - SPS	6.46	4.5 eV	3.39 eV	0.26 eV	3.65 eV
NbO <sub>2</sub> F	6.90	4.5 eV	3.36 eV	0.72 eV	4.08 eV
Nb <sub>3</sub> O <sub>7</sub> F	6.46	4.5 eV	3.54 eV	0.19 eV	3.73 eV
Nb <sub>2</sub> O <sub>5</sub>	6.22	4.5 eV	3.70 eV	-0.13 eV	3.57 eV

Especially the band gap diagram shows a significant shift of the positions of the optical bands. The shift of the conduction band towards the oxygen generation potential with no overlap to the hydrogen generation potential signifies the potential efficiency of the fluorinated semiconductors related to the water oxidation reaction.

## References

- <sup>1</sup> H. Dong, J. Sun, G. Chen, C. Li, Y. Hu, and C. Lv, *Phys. Chem. Chem. Phys.*, 2014, **16**, 23915-23921.
- <sup>2</sup> A. Habibi-Yangjeh, M. Sekofteh-Gohari, *Sep. Purif. Technol.* 2017, **184**, 334-346.
- <sup>3</sup> Z.H. Cui, and H. Jiang, *J. Phys. Chem. C*, 2017, **121**, 3241-3251.

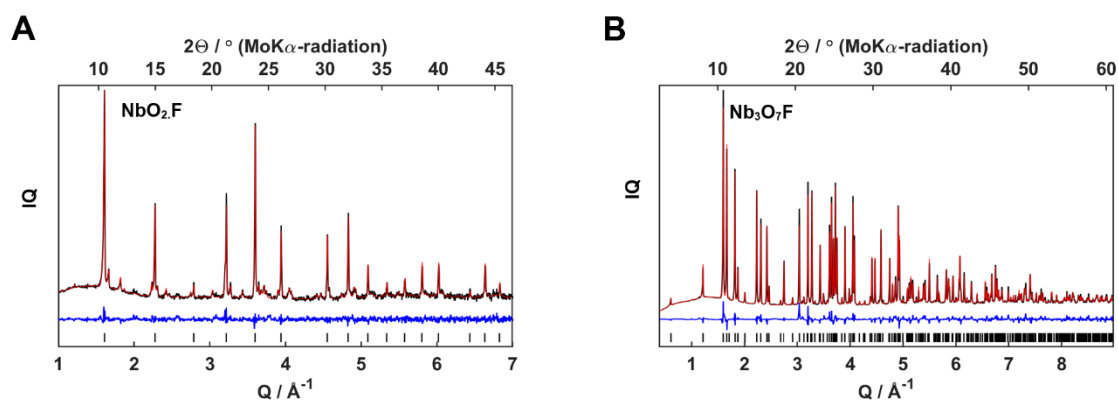


**Fig. S1.** (A) Rietveld refinement of conventionally prepared  $\text{Nb}_3\text{O}_7\text{F}$  (red line) using X-ray powder data (83 %  $\text{Nb}_3\text{O}_7\text{F}$ , 17 %  $\text{NbO}_2\text{F}$ ). (B) Rietveld refinement of conventionally prepared  $\text{Nb}_3\text{O}_7\text{F}$  (red line) using X-ray powder data. Experimental data are indicated by crosses, the calculated curve obtained after the refinement is indicated with a continuous line. The tick marks correspond to the Bragg reflections of the cubic  $\text{NbO}_2\text{F}$  and orthorhombic  $\text{Nb}_3\text{O}_7\text{F}$  structures. The continuous blue curve under the tick marks represents the difference between the experimental data and the calculated curve.



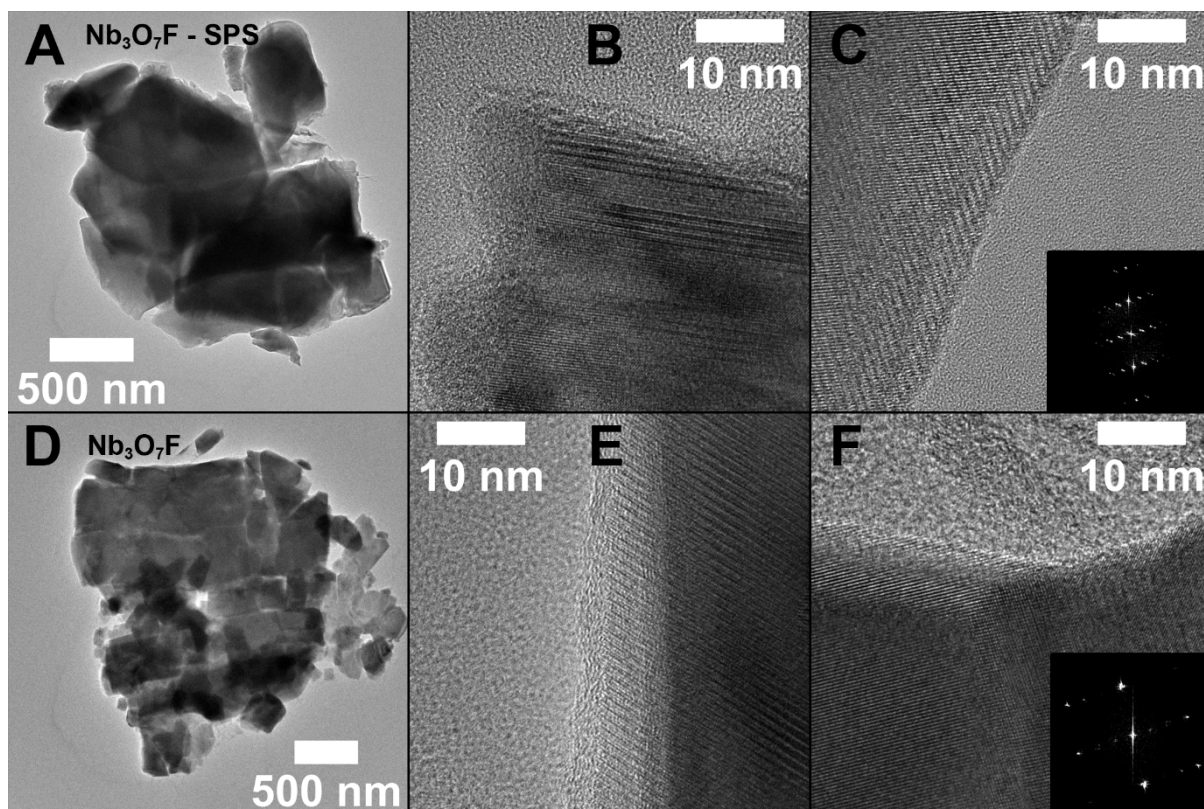


**Fig. S2.** (A-C) (HR)TEM images of  $\text{Nb}_3\text{O}_7\text{F}$  prepared by SPS, (D-F) and conventional chemistry. (A, D) show representative particles, which consist in both cases of smaller crystallites. (B, E) show a zoomed view on the edges of the layer-like particles. In case of SPS synthesis, the outer layer is larger and less crystallized than in case of conventional synthesis. (C, F) Magnified crystalline areas, which show for the SPS-prepared material less ordering and indications for twinning and disorder. The Fourier transformation (insets) exhibits diffuse intensities, which are broadened in one direction.

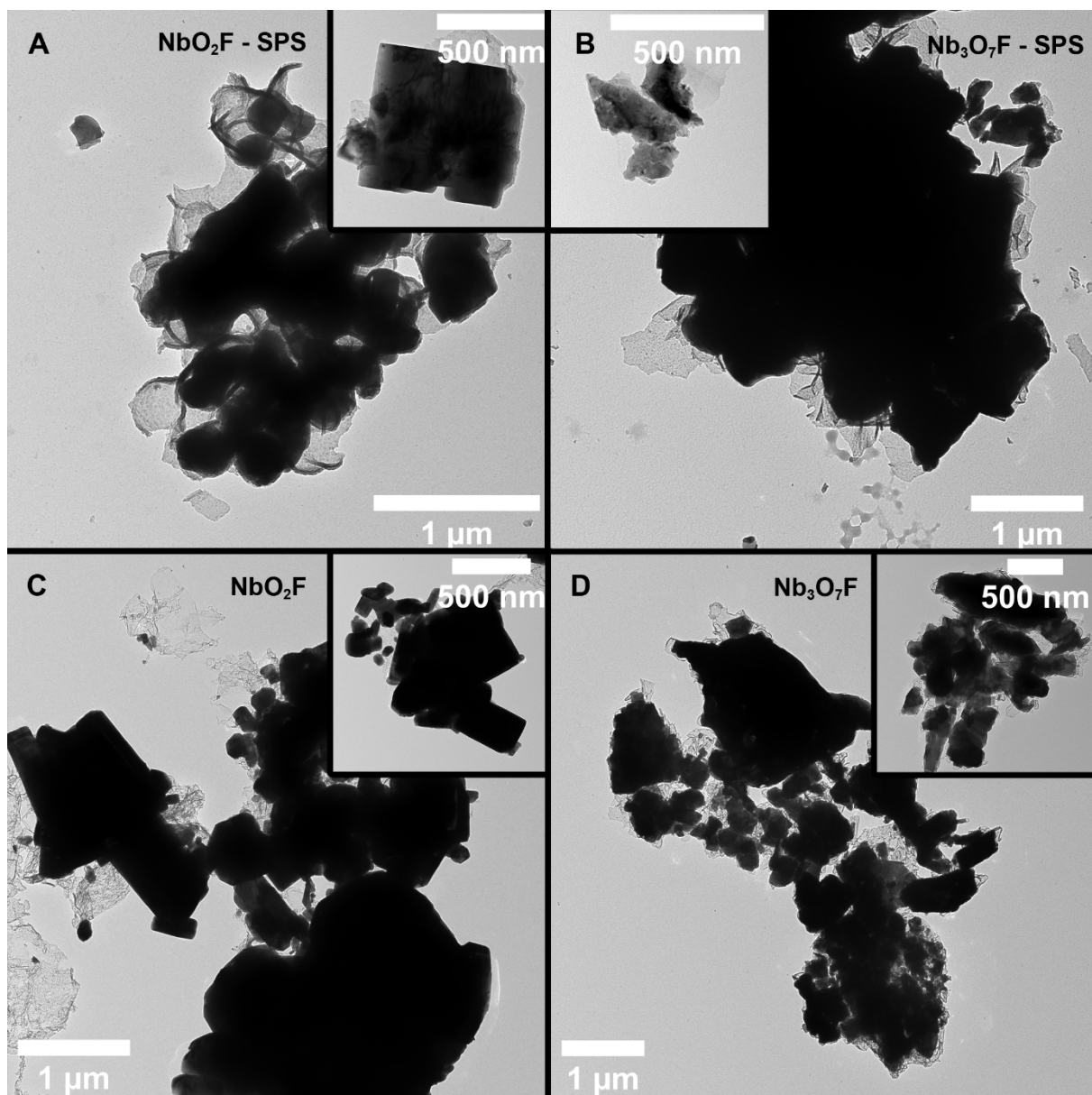


**Fig. S3.** TEM images of NbO<sub>2</sub>F and Nb<sub>3</sub>O<sub>7</sub>F prepared by SPS (**A-B**) and conventional ampoule chemistry (**C-D**). The SPS-prepared samples have similar particle size, but a more pronounced appearance of layers.

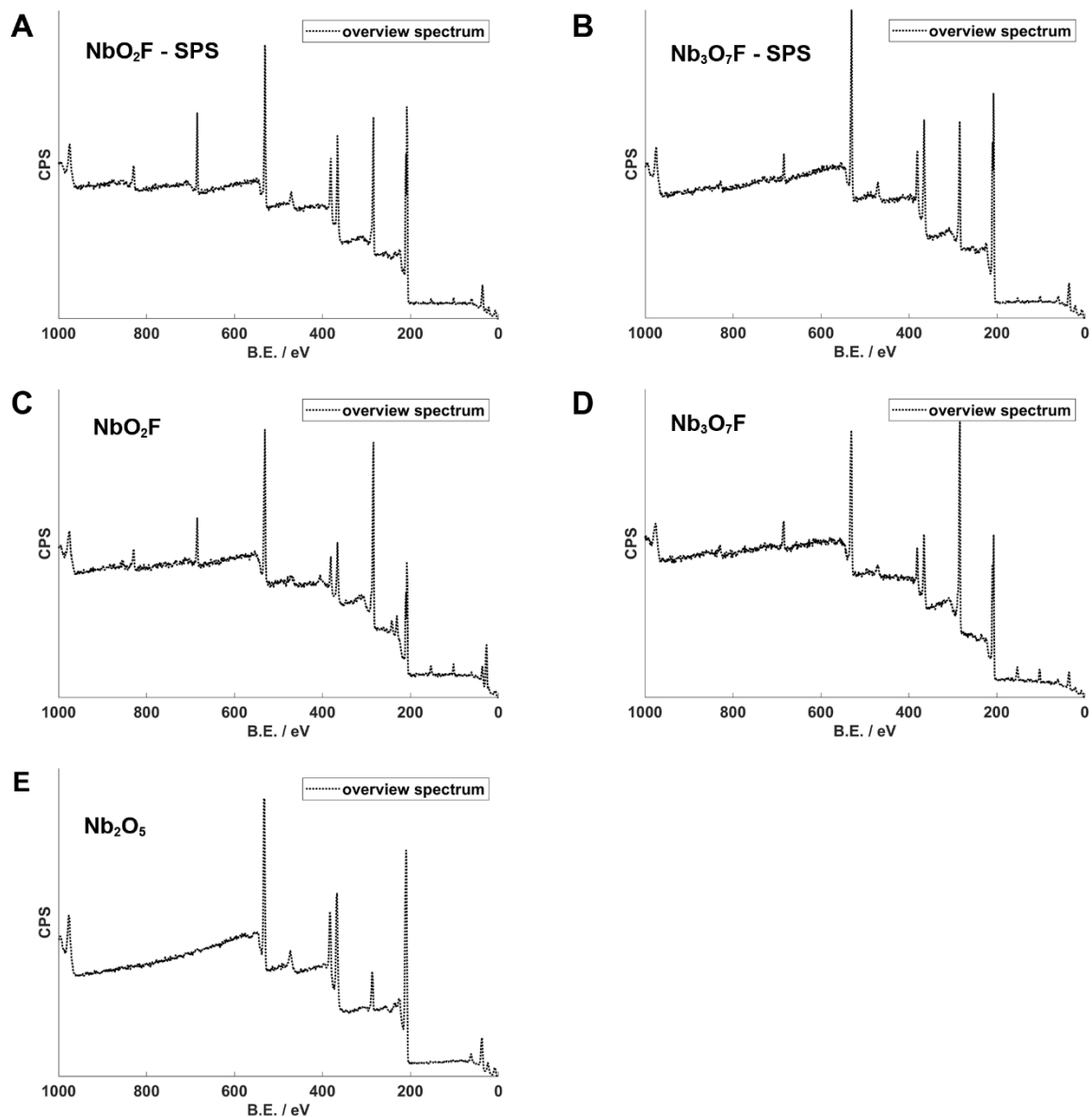


**Fig. S4.** XPS survey spectra of NbO<sub>2</sub>F and Nb<sub>3</sub>O<sub>7</sub>F, prepared by SPS (**A-B**) and conventional ampoule chemistry (**C-D**) with fitted peaks for the respective environments. (**E**) Survey spectrum of a ball-milled (unreacted) Nb<sub>2</sub>O<sub>5</sub>/PTFE reference mixture.

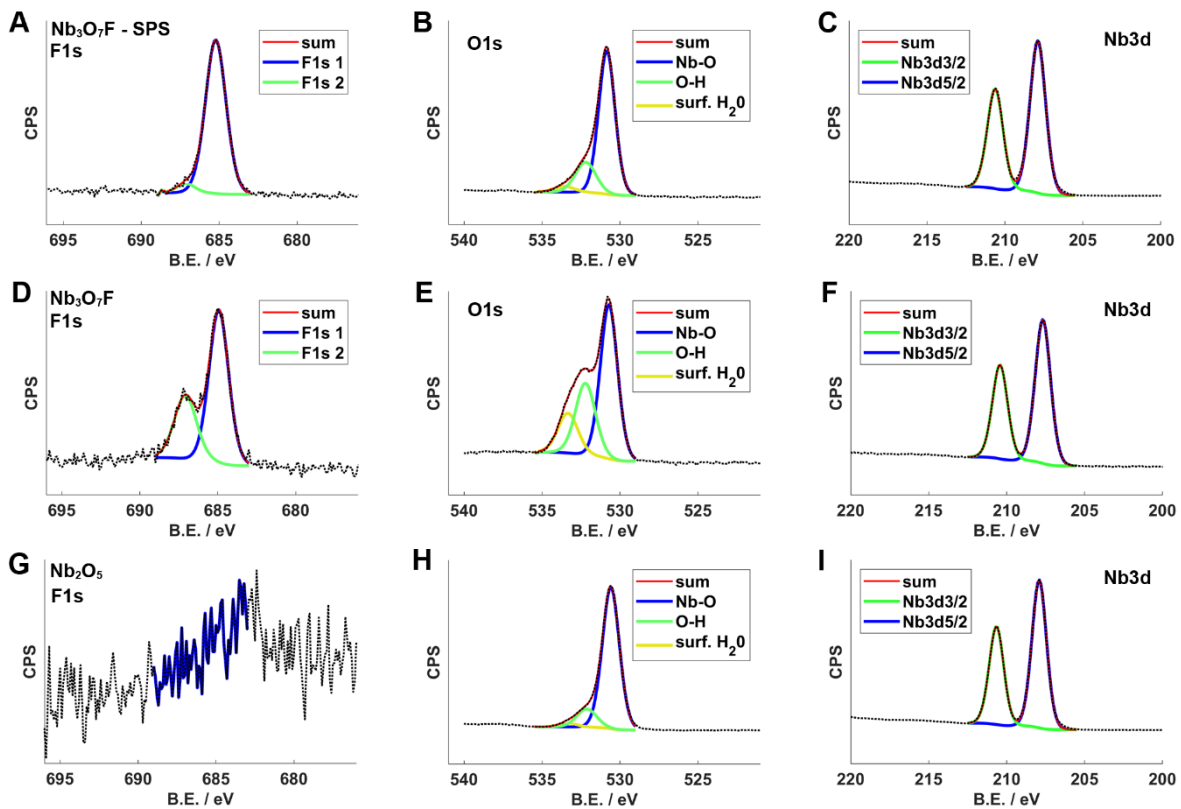


**Fig. S5.** XPS fine spectra of F, O, and Nb regimes for  $\text{Nb}_3\text{O}_7\text{F}$  prepared by SPS (A-C), conventional ampoule chemistry (D-F) and from reference  $\text{Nb}_2\text{O}_5$  (G-I, ball milled powder treated with the same SPS program as  $\text{NbO}_2\text{F}$ ) with fitted peaks for the respective environments.

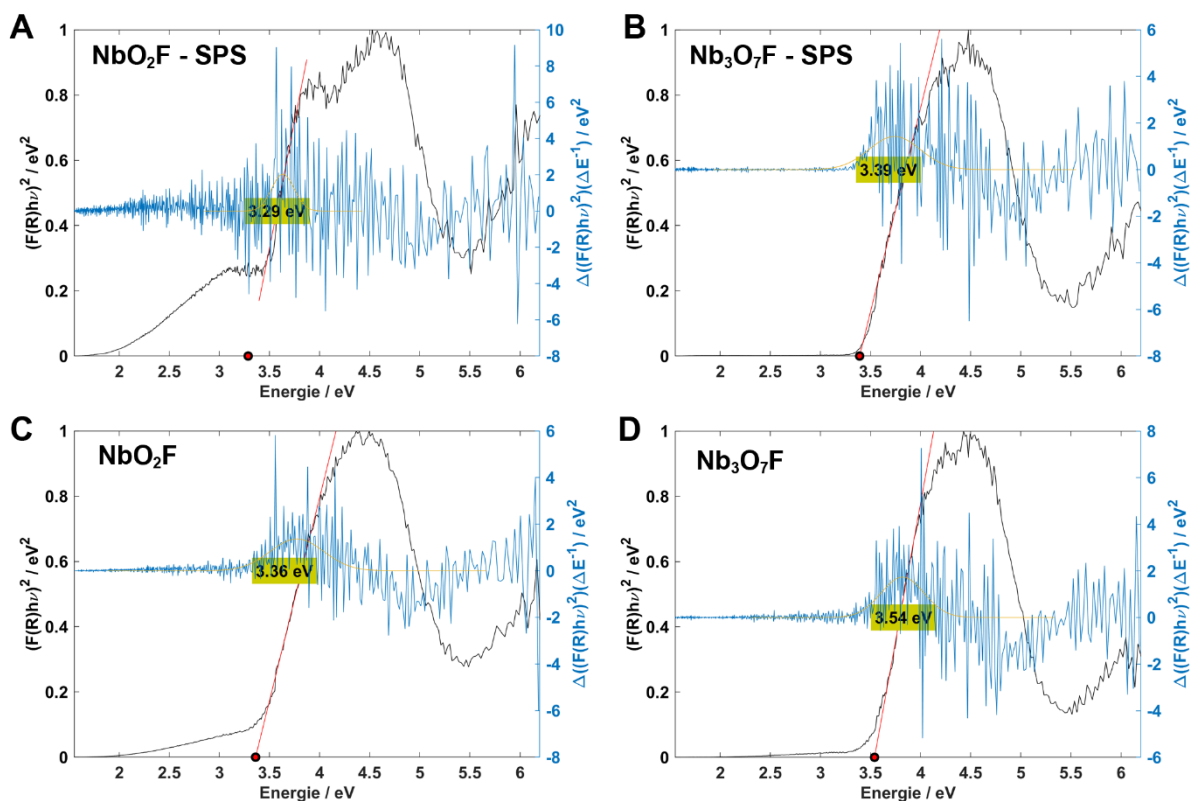


**Fig. S6.** Kubelka-Munk plots (black line) of NbO<sub>2</sub>F and Nb<sub>3</sub>O<sub>7</sub>F prepared by SPS (A-B) and conventional ampoule chemistry (C-D) from UV-Vis diffuse reflectance spectra (Fig. 5). Band-Gap values were determined by fitting the first maximum of the first derivative of the Kubelka-Munk plots (derivative - blue line, fit – yellow line) and using this value to fit the slope. Band gap values are highlighted yellow.

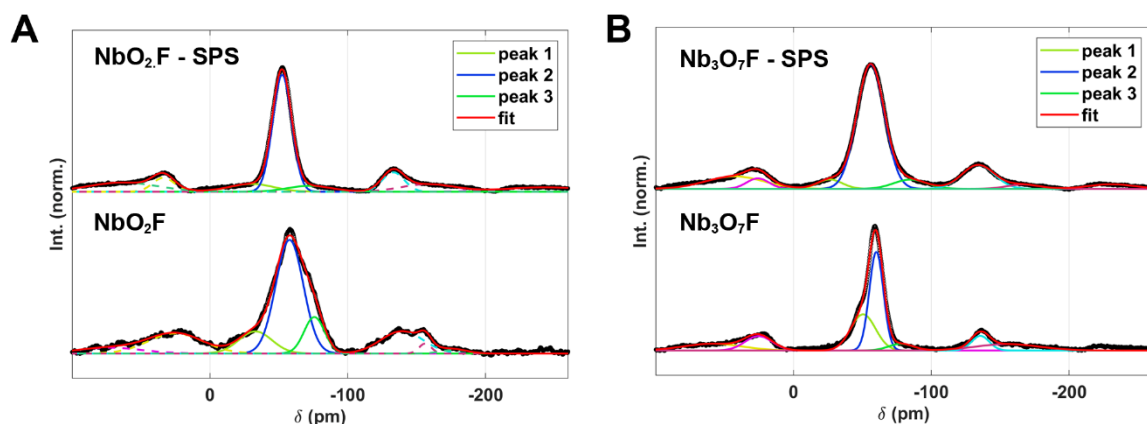


**Fig. S7.**  $^{19}\text{F}$  MAS-NMR spectra of  $\text{Nb}_3\text{O}_7\text{F}$  (A) and  $\text{NbO}_2\text{F}$  (B). In each figure the top spectrum is obtained from a SPS-prepared sample. The bottom spectrum was obtained from a conventionally prepared sample of comparable composition. Conventional prepared  $\text{NbO}_2\text{F}$  contains 17 %  $\text{Nb}_3\text{O}_7\text{F}$  as a side phase, which is the main reason for the much broader peak form as complete deconvolution of the similar signals of both phases is not possible. Potential spinning side bands are marked with stars \*.

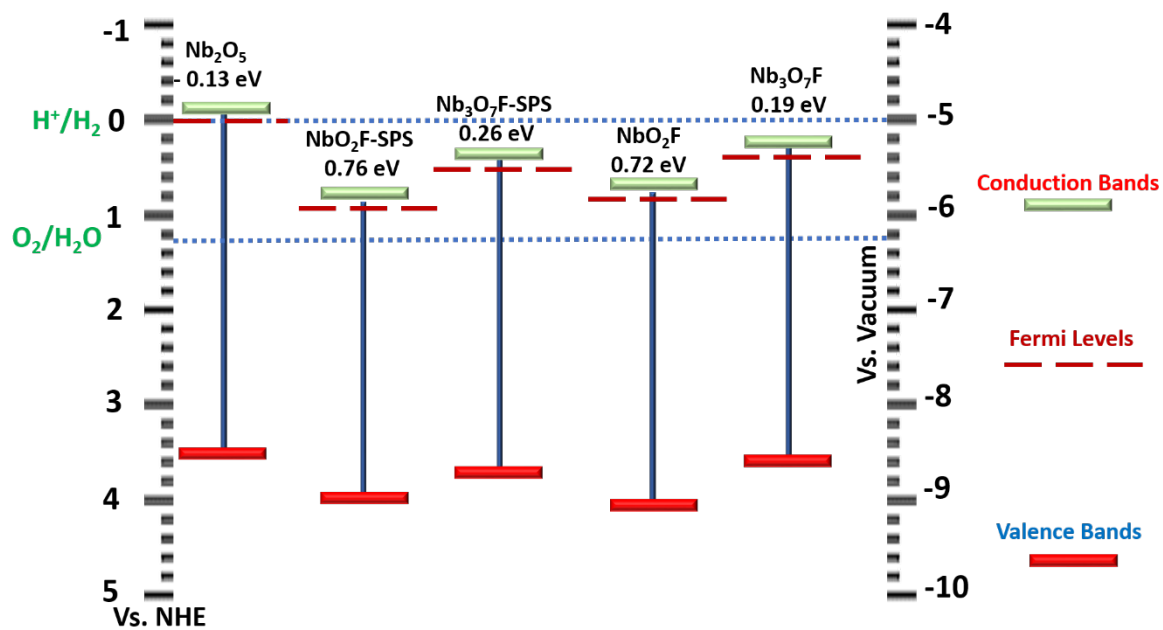


**Fig. S8.** Graphical representation of the theoretical and calculated band edge positions listed in Table S5.